

Modeling Mitral Valve Leaflets from Three-Dimensional Ultrasound

Robert J. Schneider¹, William C. Burke¹, Gerald R. Marx³,
Pedro J. del Nido², and Robert D. Howe¹

¹ Harvard School of Engineering and Applied Sciences, Cambridge, MA, USA

² Department of Cardiac Surgery, Children’s Hospital, Boston, MA, USA

³ Department of Cardiology, Children’s Hospital, Boston, MA, USA

Abstract. The geometry of the mitral leaflets, most commonly viewed using three-dimensional ultrasound, is an important input for mechanical models predicting valve closure. Current methods for leaflet modeling from ultrasound either require extensive user interaction, rely on inaccurate assumptions, or produce generic results. The presented method for modeling the mitral leaflets from three-dimensional ultrasound of an open mitral valve is automatic and able to capture patient specific geometry. The method requires as an input the location of the mitral annulus, which we generate semi-automatically using our previously designed method. No additional user interaction is required. The leaflet modeling algorithm operates by first constructing an extended surface at the location of the leaflets which extends beyond the leaflet edges into the blood pool, and then trims the surface to the observed length of the leaflets. Preliminary results suggest the leaflet modeling method, combined with our previous method for annulus segmentation, generates accurate patient-specific mitral valve models.

1 Introduction

The mitral valve is a complex three-dimensional anatomic structure which controls the blood flow between the left atrium and left ventricle in the heart. While it can be imaged using magnetic resonance or computed tomography imaging, the shape and motion of the mitral valve is most accurately captured using three-dimensional ultrasound (3DUS). Ultrasound, in addition to being inexpensive, portable, and non-ionizing, is fast enough to capture the fast moving structures of the valve. The geometry of the mitral valve is used in several applications, including mechanical modeling to predict valve closure [1, 2]. While these models typically included only generalized leaflet geometry, more recent efforts have been made to predict valve closure using patient specific geometry [2]. For this reason, several efforts have been made to model the leaflets from 3DUS.

The methods for modeling the leaflets from 3DUS can be categorized as either volumetric, mesh, or parametric. An example of a volumetric method for 3DUS was shown in [3], which used an intensity-based level set method to locate the leaflets. Unfortunately the method included not only the leaflets but anything

connected to the leaflets with similar intensity, such as the left ventricle wall, thus failing to isolate the leaflets. A method for modeling the valve as a mesh was presented in [4], which used a thin tissue detector and level sets to locate the leaflets and surrounding tissue. The method subsequently required manual intervention and the assumption of a planar annulus to construct an isolated leaflet mesh geometry. The method presented in [5] segmented and tracked the locations of several features of the mitral and aortic valve structures in 3DUS using machine learning techniques. It then fit a parametric model to the segmented locations. However, in fitting the model to only a few points, the model lacked patient-specific detail.

To compensate for the highlighted insufficiencies of previous methods, we have developed an automatic method for modeling the leaflets. The method is designed for open mitral valves because we want to differentiate between anterior and posterior leaflets, and making this distinction for coapted leaflets in 3DUS is extremely difficult even for a human observer. After finding the location of the annulus using our previously developed semi-automatic algorithm [6] and an automated optical flow tracking method based on the work by Lucas & Kanade [7], the leaflet modeling method automatically finds the location and extent of the mitral leaflets and generates a mesh to represent the geometry with no additional user interaction. We chose to represent the leaflets as a mesh because this representation can be easily used to generate either a volumetric or parametric representation if needed, is a suitable input for mechanical modeling, and is representative of the thin leaflet tissue.

The method uses the location of the annulus as a means to enforce knowledge about the location and orientation of the leaflets. The method then uses a series of steps to estimate and refine a search space coordinate system and the shape and location of the leaflets. A mesh at the location of the leaflets is then constructed as a natural consequence of the geometry of the search space. The details of the algorithm are described in Section 2. A study quantifying the performance of the method as compared to manual leaflet tracings is then shown in Section 3.

2 Methods and Materials

2.1 Algorithm Summary and Components

The mitral leaflet modeling algorithm is comprised of five main components organized in a two-pass strategy that drives the algorithm to accurately locate the leaflets (Figure 1). The components can be described as defining the search space, redefining the search space axis based on the availability of new information, estimating an extended leaflet surface using a graph cut method, refining the extended leaflet surface using an active surface method, and finally trimming the extended leaflet surface using dimensional reduction and a level set method.

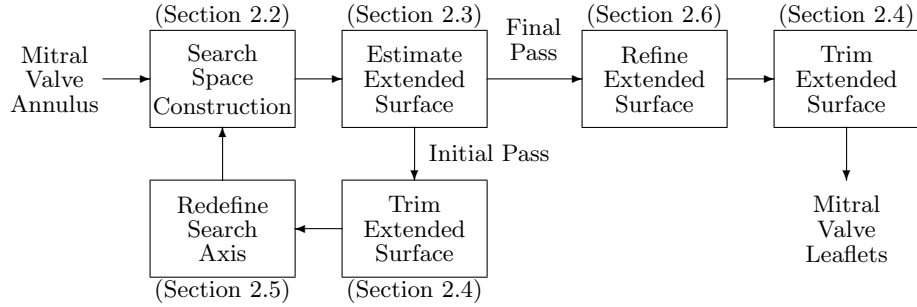


Fig. 1. Flow chart summary of the leaflet modeling algorithm. A description of each component appears in the corresponding section.

2.2 Constructing the Search Space

The location of the mitral leaflets in the heart is such that they attach to and rotate about the mitral annulus. Therefore, we search for the location of the mitral leaflets by constructing a search space that is comprised of an arc system that is centered about the annulus (Figure 2). The arcs are constructed in planes that are rotated about a defined axis. Initially, little is known about the leaflets aside from their orientation, and so the axis is generically defined as the direction of least variance as determined from a principal component analysis of the mitral annulus. For the final pass, the axis location is refined, as described in Section 2.5, to account for the estimated leaflet orientation and position. The search planes are evenly spaced at an angular offset of $\Delta\theta_p$. The arcs are evenly spaced at a radial offset of ΔR , and points are sampled along the arcs at an angular offset of $\Delta\theta_s$. The search space is designed around the assumption that the leaflets will intersect the search arcs, at most, at a single location along each arc. This point

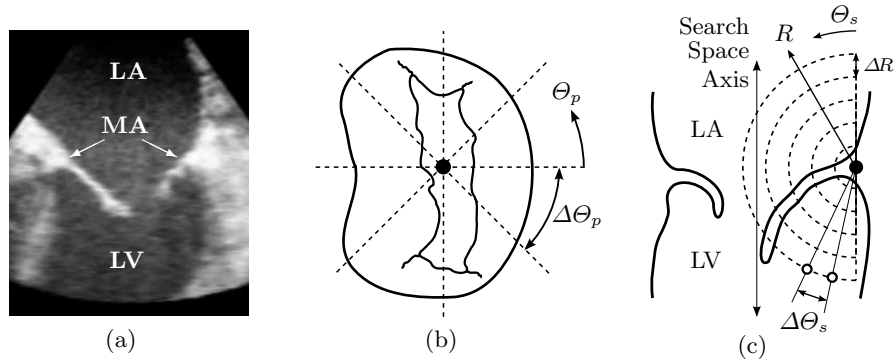


Fig. 2. Example of the location (relative to the mitral valve) and spacing of the search space axis, planes, arcs, and sample points. (a) Open mitral valve in a clinical 3DUS slice. (b) Atrial view of an open mitral valve showing search planes oriented about the search axis. (c) Cut-plane view of an open mitral valve showing the search arc and sample point configurations. (LA - left atrium; LV - left ventricle; MA - mitral annulus)

along each arc is found first using a graph-cut method to estimate the leaflet location, and in the final pass, the location is refined to account for surface curvature and the image.

2.3 Estimating an Extended Leaflet Surface

The location of the leaflets is estimated by fitting a surface to their believed location. The surface is found as the min-cut of a graph [8], where the source connects to all points at the minimum Θ_s and the sink to all points at the maximum. The undirected edges of the graph, Γ , connect neighboring points at $\Theta_p \pm \Delta\Theta_p$, $R \pm \Delta R$, and $\Theta_s \pm \Delta\Theta_s$, making Γ 6-connected. The edges of the graph have a capacity that is a function of a drive image, which is computed at each point. The drive image on the first pass is a product of the original 3DUS intensity (\mathbf{I}) and a thin tissue detector (\mathbf{TTD}) [6], $\mathbf{I}_{drv} = (\mathbf{I})(\mathbf{TTD})$. For the final pass, because we have an estimate for the leaflet location, a weighting function, \mathbf{W} , is incorporated into the drive image, $\mathbf{I}_{drv} = (\mathbf{I})(\mathbf{TTD})(\mathbf{W})$, to encourage the min-cut to be found at the estimated leaflet location. The edge capacity between points i and j is then defined as

$$E_{ij} = \frac{1}{1 + \omega (\mathbf{I}_{drv,i} + \mathbf{I}_{drv,j})^2}, \quad (1)$$

where ω is a scalar weight. The min-cut of the graph is found using Kolmogorov's implementation [9]. The point representing the leaflet surface location along each arc is herein referred to as a leaflet node.

2.4 Trimming an Extended Leaflet Surface

The extended leaflet surface should reside at the location of the leaflets and extend past the edges of the leaflets into the blood pool of the left ventricle. It is therefore necessary to trim the surface at the leaflet edge so that the remaining leaflet geometry accurately portrays the location and geometry of the mitral leaflets. The trimming operation is done by isolating the nodes that reside at the leaflets from those that reside in the blood pool. This is done by first reducing the ultrasound intensity information at the surface nodes to a two-dimensional image, where the axes of the image are the search plane angle and the arc radial offset (Figure 3). The leaflet nodes are then separated from the blood pool nodes using the RCAC level set method [3], where the level set function is initialized using a k -means algorithm. The annulus nodes are always made to be included in the leaflet group during the level set evolution, and the continuity between the first and last search plane is maintained. Nodes that are not found to be a member of the leaflet group are considered to be part of the blood pool and removed from the surface.

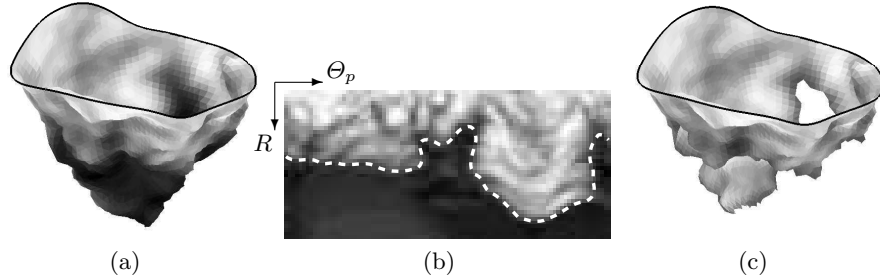


Fig. 3. (a) Example of an extended and refined leaflet surface. The gray level of the triangles reflect the 3DUS intensity. (b) The intensity image formed from the ultrasound intensity at the surface nodes. Also shown is the computed trimming contour (dashed white line) found using a level set formulation. (c) The surface from (a) that is trimmed according to the contour shown in (b). The black contours in (a) and (c) indicate the location of the mitral annulus.

2.5 Redefining the Search Space Axis

The search space axis is initially defined with only the knowledge about the general orientation of the leaflets. The problem with this generic assignment is that information about the leaflet position is unknown, and so the axis could potentially pass through the leaflet tissue, thereby creating an inconsistency in the estimated leaflet location. However, as information about the estimated leaflet location becomes available, the axis can be better defined to account for the position of the leaflets. This is done by making the axis the vector that passes through the mitral annulus center point and the center of the estimated leaflet opening. In doing so, the axis will not pass through any leaflet tissue, and will provide for a more appropriate search space in which to find the leaflets.

2.6 Refining an Extended Leaflet Surface

The min-cut algorithm is well suited for estimating the location of the extended leaflet surface, but oftentimes fails to capture finer leaflet detail. Therefore, a surface refinement method treats the surface as an active surface and drives the it toward the location of the leaflets in the image and also regulates surface curvature. In the refinement process, the nodes are restricted to move along their respective arcs in the search space. An image energy, \mathbf{E}_{img} , which is the inverse of the ultrasound intensity, drives surface nodes to the leaflet location along the arc. An internal energy, \mathbf{E}_{crv} , regulates surface curvature by driving surface nodes to locations that will result in uniform edge length. The minimized surface energy equation is then $\mathbf{E}_{surf} = \omega_{img}\mathbf{E}_{img} + \omega_{crv}\mathbf{E}_{crv}$, where ω_{img} and ω_{crv} are scalar weights.

2.7 Mesh Generation

The nodes of the trimmed leaflet surface are formed into a triangular mesh by first connecting nodes to those neighbors that exist at $\Theta_p \pm \Delta\Theta_p$ and $R \pm \Delta R$. Diagonal edges are then defined between nodes at (Θ_p, R) and $(\Theta_p + \Delta\Theta_p, R + \Delta R)$. The normals of the triangles are defined such that the positive normal direction points toward the top (atrial) side of the mitral leaflets.

3 Performance and Validation

We assessed the performance of the mitral leaflet modeling algorithm on a group of four anonymized clinical pediatric cases. The mitral valves in these cases were imaged using transesophageal echocardiography (iE33 Echocardiography System with X7-2t transesophageal probe, Philips Healthcare, Andover, MA, USA). A frame showing an open valve was manually selected from each of the four cases. The annulus, which acted as the input to the algorithm, was found using our semi-automatic annulus segmentation method [6] and a tracking algorithm based on the Lucas & Kanade method [7]. Using the location of the tracked annulus in the manually selected frame with an open valve, the leaflets were then found using the presented method.

The leaflets in the chosen frames were manually traced in cut planes taken every 10° about the search space axis and compared to the meshes generated by the algorithm (Figure 4). The intersection of the leaflet mesh with the cut planes generated contour segments in the plane. A histogram of the distances of points along these contours from the manually traced leaflet contours were then computed (Figure 5). As indicated in the histogram plot, on average 95% of the leaflet mesh points resided within 2.10mm of the manually traced leaflets, with the average distance being roughly 0.76 ± 0.65 mm. These errors were on the order of the ultrasound volume resolutions (0.5-1.0mm/voxel) and leaflet thicknesses observed in the volumes (2-3mm).

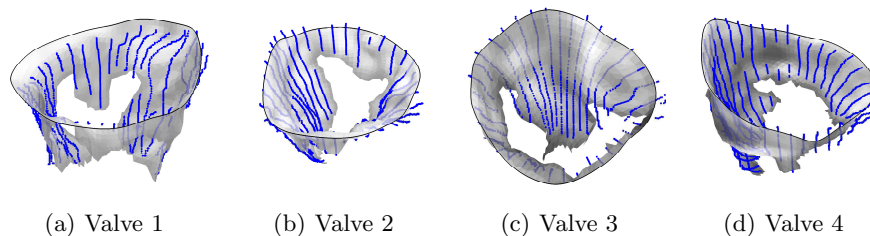


Fig. 4. Comparison of the algorithm-generated leaflet model (shaded surfaces) to manual tracings (contours) made in cut planes about the search space axis.

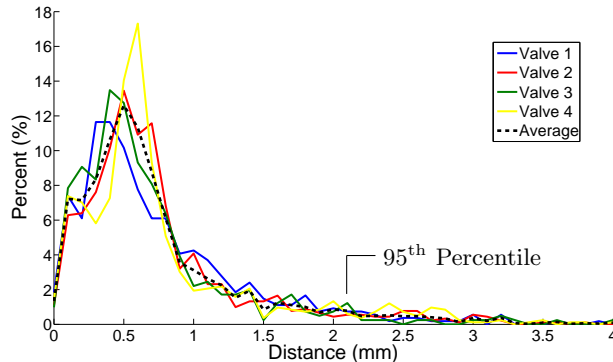


Fig. 5. Histogram of the distances of the algorithm mesh from the manually traced points in each cut plane for each valve in Figure 4 and for the group average. The 95th percentile is shown for the group average.

4 Discussion

This paper presents a method that automatically generates a model of the leaflets for an open mitral valve in a 3DUS volume given the location of the mitral annulus. The presented method differs from previous leaflet modeling methods in that it does not require extensive user interaction and generates a detailed, patient-specific leaflet mesh. The method uses a two-pass strategy that defines and refines a search space coordinate system and the leaflet surface to generate a mesh at the location of the leaflets. We showed the accuracy of this method by comparing the mesh to manual tracings of the leaflets made in cut planes taken about a designated axis, where it was found that 95% of the points along the mesh were less than 2.10mm away from the manual tracings.

The leaflet modeling is robust and accurate partly due to the fact that it exploits prior knowledge about where to find the leaflets based on the location of the mitral annulus. Accurately locating the annulus is therefore important as its location directly affects the leaflet model. To find the annulus, we first use our annulus segmentation algorithm to find the annulus in a frame with a closed valve [6]. We then track that annulus to all other frames using a modified version of the Lucas & Kanade optical flow method [7]. We compared the location of the tracked annulus to manual delineations made by three experts across 30 frames and found an average RMS error of 1.67 ± 0.63 mm between the tracked annulus and the expert mean. The accuracy of both the annulus and leaflet modeling methods makes for one of the most accurate and robust mitral valve modeling methods capable of capturing detailed patient-specific valve geometry.

A limitation of the presented leaflet modeling method is that the 3DUS images of the mitral valve need to show the leaflets as a thin structure in an open valve state. This suggests that short-axis views of the valve will not suffice, as the chordal structure that becomes visible in this approach gives the leaflets

a thick appearance. Also, the valve cannot be completely open (peak diastole) as the leaflets are pushed up against the left ventricle wall and are typically indistinguishable from the wall as seen in 3DUS. The recommended images are then those that use either an enface or apex view of the mitral valve and capture the valve during the process of opening or closing. In these views, the anterior and posterior leaflets should be differentiable.

Future work includes using the defined leaflet mesh as a geometric prior to be tracked to other frames in a 3DUS sequence to provide for a four-dimensional image-driven model of the leaflets. The benefit in this approach is that anterior and posterior mitral leaflets will be differentiated throughout a sequence, and because leaflet geometry can be preserved and collisions resolved, a coaptation line and surface should be found.

5 Acknowledgments

This work is supported by the U.S. National Institutes of Health under grant NIH R01 HL073647-06.

References

1. Kunzelman, K., Einstein, D., Cochran, R.: Fluid–structure interaction models of the mitral valve: function in normal and pathological states. *Philosophical Transactions of the Royal Society B: Biological Sciences* **362** (2007) 1393
2. Hammer, P., Perrin, D., Pedro, J., Howe, R.: Image-based mass-spring model of mitral valve closure for surgical planning. In: *Proc. SPIE - Medical Imaging*. Volume 6918. (2008) 69180Q1–8
3. Shang, Y., Yang, X., Zhu, L., Deklerck, R., Nyssen, E.: Region competition based active contour for medical object extraction. *Computerized Medical Imaging and Graphics* **32** (2008) 109–117
4. Burlina, P., Sprouse, C., DeMenthon, D., Jorstad, A., Juang, R., Contijoch, F., Abraham, T., Yuh, D., McVeigh, E.: Patient-Specific Modeling and Analysis of the Mitral Valve Using 3D-TEE. In: *Information Processing in Computer-Assisted Interventions*. Volume 6135 of *Lecture Notes in Computer Science*. (Springer) 135–146
5. Ionasec, R., Voigt, I., Georgescu, B., Wang, Y., Houle, H., Vega-Higuera, F., Navab, N., Comaniciu, D.: Patient-Specific Modeling and Quantification of the Aortic and Mitral Valves From 4-D Cardiac CT and TEE. *Medical Imaging, IEEE Transactions on* **29** (2010) 1636–1651
6. Schneider, R., Perrin, D., Vasilyev, N., Marx, G., del Nido, P., Howe, R.: Mitral Annulus Segmentation from 3D Ultrasound Using Graph Cuts. *IEEE Transactions on Medical Imaging* **29** (2010) 1676–87
7. Lucas, B., Kanade, T.: An iterative image registration technique with an application to stereo vision. In: *Proc. 7th International Joint Conference on Artificial Intelligence*, Vancouver, B.C., Canada (1981) 674–679
8. Boykov, Y., Kolmogorov, V.: An experimental comparison of min-cut/max-flow algorithms for energy minimization in vision. *IEEE Transactions on Pattern Analysis and Machine Intelligence* **26** (2004) 1124–1137
9. Kolmogorov, V.: *Software* (2004) <http://www.cs.ucl.ac.uk/staff/V.Kolmogorov/software.html>. [Accessed: October 1, 2008].